Journal of Materials Chemistry A

COMMUNICATION

View Article Online
View Journal | View Issue

Open Access Article. Published on 28 August 2015. Downloaded on 8/21/2025 9:22:38 PM.
This article is licensed under a Creative Commons Attribution 3.0 Unported Licence.

Cite this: J. Mater. Chem. A, 2015, 3, 19679

Received 27th July 2015
Accepted 28th August 2015

DOI: 10.1039/c5ta05784a

www.rsc.org/MaterialsA

The golden gate to photocatalytic hydrogen production†

Philip Kalisman,[a] Lothar Houben,‡[b] Eran Aronovitch,[c] Yaron Kauffmann,[d] Maya Bar-Sadan[c] and Lilac Amirav*[a]

We demonstrate improved efficiency for the photocatalytic water splitting reduction half reaction by employing Au–Pt bimetallic cocatalysts. We employed nanoparticle-based photocatalysts consisting of CdSe@CdS rods tipped with Au, Pt, Au–Pt core–shell or Au decorated with Pt islands. By tailoring the composition and morphology of the Au–Pt bimetallic catalysts, we achieved more than a fourfold increase in activity for hydrogen production compared to pure Pt.

Solar-driven photocatalytic splitting of water into hydrogen and oxygen is a potential source of clean and renewable fuels. Semiconductor photocatalysts are often loaded with metallic cocatalysts, which promote charge separation of photogenerated electrons and holes and also act as sites for the reduction reaction.[1,2] These cocatalysts play an essential role in reactions such as water splitting, as they offer lower activation potentials for hydrogen evolution, thereby greatly enhancing the photocatalytic activity.[3–7] The metals demonstrating the greatest catalytic performance do not necessarily form an ideal interface with the semiconductor they are grown on, resulting in less than optimal charge transfer (or accumulation). Utilization of a bimetallic catalyst may enable separate optimization of the different interfaces within such a heterostructure photocatalyst system (*i.e.* semiconductor–metal interface and metal–liquid junction).

Employing a bimetallic catalyst also extends the range of tunable properties for the metallic compounds, allowing for improved rational design of heterogeneous catalysts.[8–17] The reactivity may be tailored by changing the composition, and the exterior electronic and geometric structures of the bimetallic surfaces.[18–24] Hence, bimetallic materials are considered highly promising candidates for heterogeneous catalysis. In particular, alloys where the solid solute concentration near the surface differs from the bulk have proven quite successful.[25,26] Here we examine a combination of gold and platinum as an improved cocatalyst for the photocatalytic water splitting reduction half reaction.

Two factors differentiate bimetallic catalysts from pure metal surfaces and improve their catalytic performance: (1) the strain effect from the size-mismatch of the component metal atoms, and (2) heterometallic bonding interactions, termed the "ligand effect", between the surface atoms and the substrate. Both of these effects change the width and subsequently the energetic position of the surface d band, thereby changing the surface chemical and catalytic properties.[27] Of relevance is the dissociative adsorption energy of hydrogen, which is controlled by changes induced in the average energy of the d band.

In a semiconductor–metal photocatalytic system, the semiconductor substrate upon which the nanoscale metallic components are grown is likely to affect their electronic and geometric characteristics as well. In addition, modifications to the electronic properties of the metallic components might also affect interfacial charge-transfer processes.

We set out to examine the opportunities for improving the photocatalytic hydrogen production by coupling Pt, a known active catalyst, with Au, a metal that demonstrated the ability to accumulate charges even at the nanoscale.[28] We employed a well-controlled nanoparticle-based system for catalyzing the reduction half reaction.[29] The light absorption and excitation unit consists of a cadmium selenide (CdSe) quantum dot embedded asymmetrically within a cadmium sulfide (CdS) quantum rod.[30–32] This structure has been widely studied optically and photocatalytically and is well characterized.[33–40] The

[a]Schulich Faculty of Chemistry, Technion – Israel Institute of Technology, Haifa 32000, Israel. E-mail: lilac@technion.ac.il

[b]Peter Grünberg Institut 5 and Ernst Ruska-Centre for Microscopy and Spectroscopy with Electrons, Forschungszentrum Jülich GmbH, 52425 Jülich, Germany

[c]Department of Chemistry, Ben-Gurion University of the Negev, Beer-Sheva, Israel

[d]Department of Materials Science & Engineering, Technion-Israel Institute of Technology, Haifa 32000, Israel

† Electronic supplementary information (ESI) available: Includes detailed description of the typical preparation of the different metal decorated CdSe@CdS nanorods, and techniques used in characterization of these particles. See DOI: 10.1039/c5ta05784a

‡ Current address: Chemical Research Support, Weizmann Institute of Science, Rehovot, Israel.

Open Access Article. Published on 28 August 2015. Downloaded on 8/21/2025 9:22:38 PM.
This article is licensed under a Creative Commons Attribution 3.0 Unported Licence.

pure metals, Au and Pt, and different combinations thereof, were grown onto nanorods forming a single catalytic reduction site, as can be seen in Fig. 1.

Growth of the metal tips was attained with photodeposition, using procedures loosely based on previous protocols for deposition of Pt[41] and Au.[42] Photodeposition was preferred over colloidal growth[43,44] as it allows for metal deposition at room temperature. It is presumed that such moderate growth conditions are necessary for the formation of well-controlled structures. Noteworthy is the fact that despite the use of a seeded rod as the semiconductor substrate, the metal catalyst was deposited almost exclusively at the tip, rather than along the side of the rod, adjacent to the seed, as was previously observed for similar structures.[41,42,45]

In addition to pure metals that were examined for comparison, sets of different compositions of Au–Pt bimetallic tips were made. This included Pt deposition on premade Au tips (Au@Pt), and codeposition of Au and Pt (varying the relative precursor amounts and growth time). Each set was grown on the same sample of CdSe@CdS rods, and great care was devoted to insuring that the composition of the metal tip was the only altered parameter.

We examined the activity of these sets of rods towards hydrogen production. Solutions of rods suspended in water with IPA (10% by volume) acting as a hole scavenger were placed in a home made gas-tight reaction cell purged with argon. The samples were then illuminated with a 455 nm LED adjusted to 50 mW (a photon flux of 1.15×10^{17} photons per second). The evolved hydrogen was analyzed using an online gas chromatograph equipped with a thermal conductivity detector. The apparent quantum efficiency of the sample, which is defined as $QE = 2N_{H_2}/N_{h\nu}$ was determined by quantifying the amount of evolved hydrogen at a given photon flux. The results for a representative set are presented in Fig. 2.

It is important to note that the absolute activity of the sample is strongly related to the rod morphology.[29] Here we worked with 30–40 nm long rods that do not realize the system's full potential for hydrogen production, but allow for improved elemental analysis of the tip. Hence, only relative evaluation of the activity is given significance for these sets.

As expected, rods decorated with a Au cocatalyst showed very low activity, compared to rods with a Pt cocatalyst. When a preformed Au tip was coated with Pt the activity towards hydrogen production improved further, resulting in a twofold increase compared to pure Pt. This improved activity can be explained by the reasoning described in the introduction. Furthermore, Yu *et al.* reported recently that the injection of photoinduced electrons from CdSe nanorods into a Au tip is faster than their injection into a Pt tip, but only Pt can completely extract the excited electrons from the semiconductor nanorod.[46] Consequently, the combination of the two metals is expected to enable both fast and efficient charge transfer, as required for hydrogen production.

Interestingly, the highest activity for the reduction half reaction, with more than a fourfold increase compared to pure Pt, was obtained from the sample in which the two metals were deposited simultaneously.

In order to better understand the structure-property relationship these hybrid nanostructures were characterized at the atomic level. Given the size of the metal tip (ranging from 2 to 4 nm) and a similar Z contrast of Pt and Au, we focused on elemental mapping with X-ray energy dispersive spectroscopy (EDS), for the analysis of the composition. The results, which are presented in Fig. 3, indicate that for the bimetallic tip that was grown with simultaneous codeposition of Au and Pt, a core of Au decorated with islands of Pt was formed.

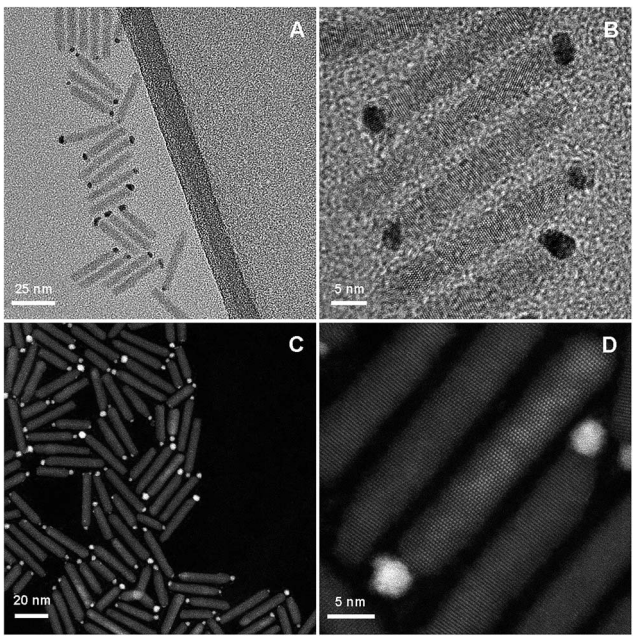

Fig. 1 TEM (A and B) and HAADF (C and D) micrographs of CdSe@CdS nanorod photocatalysts with Au–Pt bimetallic tips acting as cocatalyst reduction sites.

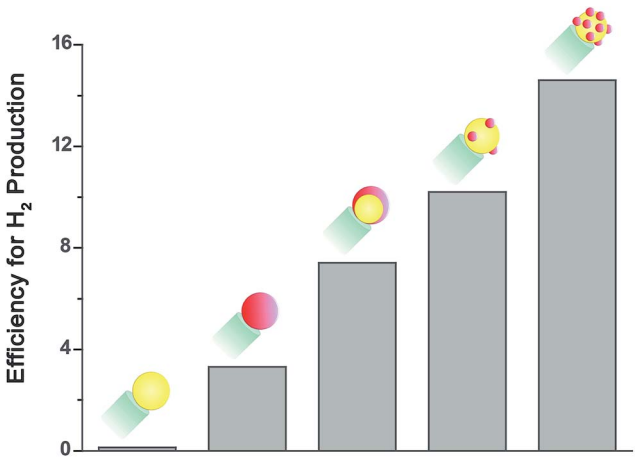

Fig. 2 Relative efficiency for the photocatalytic hydrogen production half reaction utilizing CdSe@CdS nanorods decorated with different metal cocatalysts serving as reduction sites: Au (yellow), Pt (red), Au@Pt core–shell and Au–Pt. All measurements were done under identical solution conditions, and at equivalent concentrations.

 This journal is © The Royal Society of Chemistry 2015

Open Access Article. Published on 28 August 2015. Downloaded on 8/21/2025 9:22:38 PM.
This article is licensed under a Creative Commons Attribution 3.0 Unported Licence.

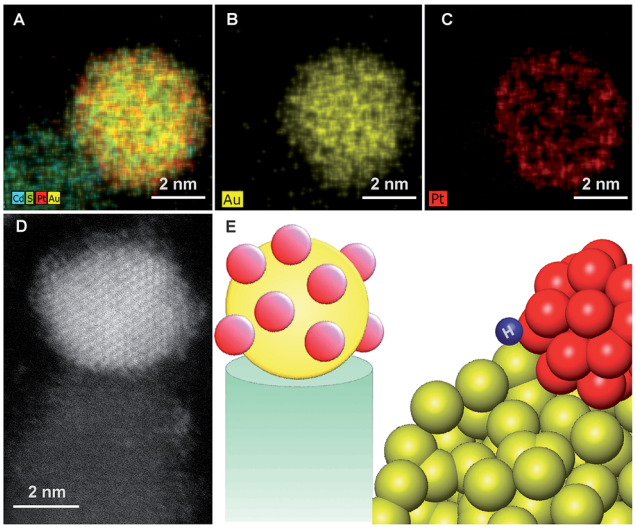

Fig. 3 X-ray energy dispersive spectroscopy micrographs with elemental mapping (A–C) and an atomic resolution HAADF image (D) of the bimetallic tip, demonstrating the formation of a Au core that is decorated with islands of Pt (E). The Au–Pt boundary is suggested to be the active catalytic site.

The bulk phase diagram of Au/Pt shows limited miscibility of the two metals.[47] The degree of segregation and atomic ordering in nanoscale alloys depends on multiple factors, mainly bond strengths, surface energetics, and atomic sizes.[48] Since the Au–Pt bonds are not sufficiently strong compared to Au–Au and Pt–Pt, segregation is favored. Typically, the species forming the strongest homonuclear bonds tends to be at the core of the nanoparticle, while the element with the lowest surface energy tends to segregate to the surface. The observed atomic arrangement for this particular Au–Pt nanoparticle depends critically on the balance of the factors outlined above, as well as on the preparation method and experimental conditions. The bimetallic nanoparticle is supported by the CdS rod on one side and is passivated by ligands on the other. The strength of binding to the support or ligands will also affect the atomic order. The Au core–Pt shell arrangement is consistent with the fact that Au is more noble and hence easier to reduce than Pt, making this the kinetic product, though surface and cohesive energy would favor the reverse configuration.[49,50]

While bulk Au–Pt alloys exhibit a miscibility gap, Chen *et al.* report that Au–Pt surface alloys may exhibit a series of ordered striped structures, due to the competition between the energy penalty of Au–Pt bonds at the boundaries and strain relaxation.[51] This is consistent with the observed formation of Pt islands, which decorate the Au core.

Of significance is the reported effect of lateral heterogeneity. A strong correlation was found between oxygen binding energy and the local Au/Pt environment of the surface adsorbate.[51] DFT calculations indicate that CO binds strongly to both the Pt and Au atoms, with the strongest binding being to Pt atoms that are adjacent to Au.[52] This was reflected in high activity of Pt–Au nanoalloys for the electrocatalytic oxidation of CO.[53] Hence, we suggest that the unique morphology of the Au core decorated with Pt islands, which introduces numerous exposed interfaces between the two phases, contributes to the improved activity towards hydrogen production.

Privman and co-workers applied a kinetic Monte Carlo model to the shell formation in core–shell particle synthesis. They observed formation of cluster-structured, or smooth epitaxial shells that are formed at a higher temperature.[54] We thus suggest that the control over tip morphologies was made possible by the flexibility of photochemical deposition, and the moderate growth conditions it allows. Millstone,[55] Khashab,[56] Goia[57] and their co-workers reported recently on alternative strategies for the formation of organized decoration of Au nanosubstrates with Pt nanoparticles. Here, we demonstrate that this synthetic effort is advantageous also for photocatalysis.

Conclusions

Building a golden gate through which electrons can migrate from the semiconductor photocatalyst to the Pt cocatalyst islands results in increased activity for the water reduction half reaction.

Acknowledgements

This research was carried out in the framework of Russell Berrie Nanotechnology Institute (RBNI) and the Nancy and Stephen Grand Technion Energy Program (GTEP). The authors acknowledge the generous support from the I-CORE Program of the Planning and Budgeting Committee, and The Israel Science Foundation (Grant No. 152/11), as well as the Adelis Foundation support in research in renewable energy. We thank the Schulich Faculty of Chemistry and the Technion – Israel Institute of Technology for the renovated laboratory and startup package. P.K. acknowledges the Schulich postdoctoral fellowship for their support. M.B.S. and E.A. gratefully acknowledge ISF grant 475/12. The access to the ER-C and the aberration-corrected instruments was granted through the European Union Seventh Framework Program, under Grant Agreement 312483-ESTEEM2 (Integrated Infrastructure Initiative-I3).

Notes and references

1 T. Sakata, T. Kawai and K. Hashimoto, *Chem. Phys. Lett.*, 1982, **88**, 50–54.
2 D. E. Aspnes and A. Heller, *J. Phys. Chem.*, 1983, **87**, 4919–4929.
3 S. Trasatti, *J. Electroanal. Chem.*, 1972, **39**, 163–184.
4 S. Sato and J. M. White, *Chem. Phys. Lett.*, 1980, **72**, 83–86.
5 P. V. Kamat, *Chem. Rev.*, 1993, **93**, 267–300.
6 A. L. Linsebigler, G. Q. Lu and J. T. Yates, *Chem. Rev.*, 1995, **95**, 735–758.
7 K. Maeda, K. Teramura, D. Lu, T. Takata, N. Saito, Y. Inoue and K. Domen, *Nature*, 2006, **440**, 295.
8 C. H. Christensen and J. K. Norskov, *J. Chem. Phys.*, 2008, **128**, 182503.

Open Access Article. Published on 28 August 2015. Downloaded on 8/21/2025 9:22:38 PM.
This article is licensed under a Creative Commons Attribution 3.0 Unported Licence.

9 F. Tao, M. E. Grass, Y. W. Zhang, D. R. Butcher, J. R. Renzas, Z. Liu, J. Y. Chung, B. S. Mun, M. Salmeron and G. A. Somorjai, *Science*, 2008, **322**, 932–934.
10 C. A. Menning and J. G. Chen, *J. Chem. Phys.*, 2008, **128**, 164703.
11 Y. Xu, A. V. Ruban and M. Mavrikakis, *J. Am. Chem. Soc.*, 2004, **126**, 4717–4125.
12 Y. G. Ma and P. B. Balbuena, *J. Phys. Chem. C*, 2008, **112**, 14520.
13 O. M. Lovvik and S. M. Opalka, *Surf. Sci.*, 2008, **602**, 2840–2844.
14 J. R. Kitchin, K. Reuter and M. Scheffler, *Phys. Rev. B: Condens. Matter Mater. Phys.*, 2008, **77**, 075437.
15 R. Callejas-Tovar and P. B. Balbuena, *Surf. Sci.*, 2008, **602**, 3531–3539.
16 V. Soto-Verdugo and H. Metiu, *Surf. Sci.*, 2007, **601**, 5332–5339.
17 J. Greeley, T. F. Jaramillo, J. Bonde, I. B. Chorkendorff and J. K. Norskov, *Nat. Mater.*, 2006, **5**, 909–913.
18 W. Chen, W. F. Schneider and C. Wolverton, *J. Phys. Chem. C*, 2014, **118**, 8342–8349.
19 J. K. Norskov, T. Bligaard, J. Rossmeisl and C. H. Christensen, *Nat. Chem.*, 2009, **1**, 37–46.
20 J. Greeley, J. K. Norskov and M. Mavrikakis, *Annu. Rev. Phys. Chem.*, 2002, **53**, 319–348.
21 J. R. Kitchin, J. K. Norskov, M. A. Barteau and J. G. Chen, *Catal. Today*, 2005, **105**, 66–73.
22 V. R. Stamenkovic, B. S. Mun, M. Arenz, K. J. J. Mayrhofer, C. A. Lucas, G. F. Wang, P. N. Ross and N. M. Markovic, *Nat. Mater.*, 2007, **6**, 241–247.
23 J. Greeley and M. Mavrikakis, *Nat. Mater.*, 2004, **3**, 810–815.
24 R. Su, R. Tiruvalam, A. J. Logsdail, Q. He, C. A. Downing, M. T. Jensen, N. Dimitratos, L. Kesavan, P. P. Wells, R. Bechstein, H. H. Jensen, S. Wendt, C. R. A. Catlow, C. J. Kiely, G. J. Hutchings and F. Besenbacher, *ACS Nano*, 2014, **8**, 3490–3497.
25 A. U. Nilekar and M. Mavrikakis, *Surf. Sci.*, 2008, **602**, L89–L94.
26 K. Hartl, K. J. J. Mayrhofer, M. Lopez, D. Goia and M. Arenz, *Electrochem. Commun.*, 2010, **12**, 1487–1489.
27 J. R. Kitchin, J. K. Norskov, M. A. Barteau and J. G. Chen, *Phys. Rev. Lett.*, 2004, **93**, 156801.
28 R. Costi, A. E. Saunders, E. Elmalem, A. Salant and U. Banin, *Nano Lett.*, 2008, **8**, 637–641.
29 L. Amirav and A. P. Alivisatos, *J. Phys. Chem. Lett.*, 2010, **1**, 1051–1054.
30 D. V. Talapin, R. Koeppe, S. Gotzinger, A. Kornowski, J. M. Lupton, A. L. Rogach, O. Benson, J. Feldmann and H. Weller, *Nano Lett.*, 2003, **3**, 1677–1681.
31 D. V. Talapin, J. H. Nelson, E. V. Shevchenko, S. Aloni, B. Sadtler and A. P. Alivisatos, *Nano Lett.*, 2007, **7**, 2951–2959.
32 L. Carbone, C. Nobile, M. de Giorgi, F. Della Sala, G. Morello, P. Pompa, M. Hytch, E. Snoeck, A. Fiore, I. R. Franchini, M. Nadasan, A. F. Silvestre, L. Chiodo, S. Kudera, R. Cingolani, R. Krahne and L. Manna, *Nano Lett.*, 2007, **7**, 2942–2950.
33 C. She, A. Demortiere, E. V. Shevchenko and M. Pelton, *J. Phys. Chem. Lett.*, 2011, **2**, 1469–1475.
34 K. Wu, W. E. Rodrıguez-Cordoba, Z. Liu, H. Zhu and T. Lian, *ACS Nano*, 2013, **7**, 7173–7185.
35 H. Zhu, N. Song, H. Lv, C. L. Hill and T. Lian, *J. Am. Chem. Soc.*, 2012, **134**, 11701–11708.
36 K. Tarafder, Y. Surendranath, J. H. Olshansky, A. P. Alivisatos and L. W. Wang, *J. Am. Chem. Soc.*, 2014, **136**, 5121–5131.
37 K. Wu, Z. Chen, H. Lv, H. Zhu, C. L. Hill and T. Lian, *J. Am. Chem. Soc.*, 2014, **136**, 7708–7716.
38 A. Demortiere, R. D. Schaller, T. Li, S. Chattopadhyay, G. Krylova, T. Shibata, P. C. dos Santos Claro, C. E. Rowland, J. T. Miller, R. Cook, B. Lee and E. V. Shevchenko, *J. Am. Chem. Soc.*, 2014, **136**, 2342–2350.
39 K. Wu, H. Zhu and T. Lian, *Acc. Chem. Res.*, 2015, **48**, 851–859.
40 E. Khon, K. Lambright, R. S. Khnayzer, P. Moroz, D. Perera, E. Butaeva, S. Lambright, F. N. Castellano and M. Zamkov, *Nano Lett.*, 2013, **13**, 2016–2023.
41 G. Dukovic, M. G. Merkle, J. H. Nelson, S. M. Hughes and A. P. Alivisatos, *Adv. Mater.*, 2008, **20**, 4306–4311.
42 G. Menagen, J. E. Macdonald, Y. Shemesh, I. Popov and U. Banin, *J. Am. Chem. Soc.*, 2009, **131**, 17406–17411.
43 T. Mokari, E. Rothenberg, I. Popov, R. Costi and U. Banin, *Science*, 2004, **304**, 1787–1790.
44 S. E. Habas, P. D. Yang and T. Mokari, *J. Am. Chem. Soc.*, 2008, **130**, 3294–3295.
45 M. G. Alemseghed, T. P. A. Ruberu and J. Vela, *Chem. Mater.*, 2011, **23**, 3571–3579.
46 P. Yu, X. Wen, Y. C. Lee, W. C. Lee, C. C. Kang and J. Tang, *J. Phys. Chem. Lett.*, 2013, **4**, 3596–3601.
47 H. Okamoto and T. B. Massalski, *Bull. Phase Alloy Diagr.*, 1985, **6**, 46–56.
48 R. Ferrando, J. Jellinek and R. L. Johnston, *Chem. Rev.*, 2008, **108**, 845–910.
49 L. M. Liz-Marzán and A. P. Philipse, *J. Phys. Chem.*, 1995, **99**, 15120.
50 M. J. Bradley, C. G. Read and R. E. Schaa, *J. Phys. Chem. C*, 2015, **119**, 8952–8959.
51 W. Chen, D. Schmidt, W. F. Schneider and C. Wolverton, *J. Phys. Chem. C*, 2011, **115**, 17915–17924.
52 Q. Ge, C. Song and L. Wang, *Comput. Mater. Sci.*, 2006, **35**, 247–253.
53 M. M. Maye, Y. B. Lou and C. J. Zhong, *Langmuir*, 2000, **16**, 7520–7523.
54 V. Gorshkov, V. Kuzmenko and V. Privman, *J. Phys. Chem. C*, 2014, **118**, 24959–24966.
55 P. J. Straney, L. E. Marbella, C. M. Andolina, N. T. Nuhfer and J. E. Millstone, *J. Am. Chem. Soc.*, 2014, **136**, 7873–7876.
56 H. M. Song, D. H. Anjum, R. Sougrat, M. N. Hedhili and N. M. Khashab, *J. Mater. Chem.*, 2012, **22**, 25003–25010.
57 R. K. Roy, J. I. Njagi, B. Farrell, I. Halaciuga, M. Lopez and D. V. Goia, *J. Colloid Interface Sci.*, 2012, **369**, 91–95.

 This journal is © The Royal Society of Chemistry 2015